Fluid Structure Interaction Analysis for Prediction of Centrifugal Compressor Dynamic Stresses

Kevin Hoopes
Senior Research Engineer
Southwest Research Institute
San Antonio, TX, USA

Charles Leavitt
Senior Structural Analyst
Elliott Group
Jeannette, PA, USA

Aaron Rimpel
Group Leader
Southwest Research Institute
San Antonio, TX, USA

Tim Allison
Director-R&D
Southwest Research Institute
San Antonio, TX, 78253

Klaus Brun
Director, Research and Development
Elliott Group
Jeannette, PA, USA

Ronald Josefczyk
Director, Global Engineering
Elliott Group
Jeannette, PA, USA

Mr. Kevin Hoopes is a Senior Research Engineer in the Rotating Machinery Dynamics Section at Southwest Research Institute in San Antonio Texas. Mr. Hoopes joined SwRI in 2013 after completing his M.S. degree in Mechanical Engineering from Virginia Tech. His interests include aerodynamics, thermodynamics, heat transfer, fluid dynamics, turbomachinery, and digital manufacturing. In these areas, Mr. Hoopes is especially interested in numerical simulation and physics based design optimization of turbomachinery and related components.

Mr. Charles Leavitt is a Senior Structural Analyst in the Engineered Products Department at Elliott Group in Jeannette, PA, where he has been for six years. His expertise includes static and dynamic structural mechanics and computational fluid dynamics. Mr. Leavitt earned his Master of Science degree in Mechanical Engineering from Carnegie Mellon University.

Mr. Aaron Rimpel is a Group Leader in the Rotating Machinery Dynamics Section of the Machinery Department at Southwest Research Institute in San Antonio, TX, where he has been for ten years. His expertise is in mechanical system design, rotordynamics, and development of rigs for testing bearings and seals for conventional and oil-free machinery. Mr. Rimpel earned his Master of Science degree in Mechanical Engineering from Texas A&M University with a focus on rotordynamics and gas bearings.

Dr. Tim Allison is the Machinery Department Director at Southwest Research Institute where he leads an organization that focuses on R&D for the energy industry. His research experience includes analysis, fabrication, and testing of turbomachinery and systems for advanced power or oil & gas applications including high-pressure turbomachinery, centrifugal compressors, expanders, gas turbines, reciprocating compressors, and test rigs for bearings, seals, blade dynamics, and aerodynamic performance. Dr. Allison has authored over 60 papers, published four book chapters, is a past chairman of the ASME Oil & Gas Applications Committee, and an Associate Editor for the ASME Journal of Engineering for Gas Turbines & Power

Dr. Brun is the Director of Research & Development at Elliott Group where he leads a group of over 60 professionals in the development of turbomachinery and related systems for the energy industry. His past experience includes positions in product development, applications engineering, project management, and executive management at Southwest Research Institute, Solar Turbines, General Electric, and Alstom. He holds ten patents, has authored over 350 papers, and published four textbooks on energy systems and turbomachinery.

Mr. Ronald Josefczyk is the Director of Global Engineering at Elliott Group, Ebara Corporation where he has responsibility for all aspects of application engineering, design, manufacturing and testing of centrifugal and axial compressors, steam turbines and hot gas expanders for all Engineered Products globally. Mr. Josefczyk has previously held roles of Director of Research & Development, Product Manager and Consulting Engineer positions with Elliott Group and Product Engineer with GE Oil and Gas. He holds two turbomachinery patents and received his B.S. degree in Mechanical Engineering from the University of Pittsburgh.

ABSTRACT

Centrifugal compressor impellers experience dynamic loading from flow structures generated by upstream and downstream compressor components. This loading can cause high cycle fatigue and ultimately impeller failure if not accounted for during the design of the impeller. This paper reviews the use of Fluid Structure Interaction as a method for the prediction of these unsteady pressures and resultant dynamic stresses. This paper describes a recent analysis effort to predict dynamic pressures and aerodynamic damping in an industrial centrifugal compressor application. Specific fluid meshing and solution strategies are discussed including a direct time dependent full 360 degree sliding mesh solution and a single passage pitch change solution, using either a Time Transformation or a Fourier Transformation method. Also discussed is the methodology for imposing dynamic pressures from a computational fluid dynamic (CFD) analysis on a forced harmonic structural response analysis to predict unsteady impeller stresses. Particular attention is paid to the post processing of the predicted stress field to inform a prediction of the acceptability of the fatigue performance of the impeller.

INTRODUCTION

Centrifugal compressors often use components upstream of an impeller, such as guide vanes, to control swirl velocities at the impeller inlet. The presence of the guide vanes introduces flow field variations, i.e. guide vane wakes, which vary around the circumference of the flow path at the impeller inlet. As an impeller blade rotates through each guide vane's wake it experiences a variation of the pressures acting upon the blades. The frequency of the variation is a function of the impeller rotation speed and the number of upstream guide vanes. Normally these variations do not cause significant stress in the impeller and are of little concern. However, if the frequency of the pressure variations coincides with or is near to the frequency of a structural natural vibration mode of the impeller, there is the potential of dynamic amplification of the impeller's structural response, i.e resonance. The magnitude of the resulting resonant response depends upon the strength of the forcing function (pressure variations), the degree that the spatial distribution of the pressure variations coincides with the structural mode shape and the level of aerodynamic and structural damping present. The resulting dynamically amplified response stresses are still not typically of a magnitude for concern with regard to sudden failure of the impeller, i.e. ductile or brittle fracture. However, the impeller experiences a stress cycle with each guide vane wake passing resulting in a very large number of stress cycles. This becomes a potential concern with regard to high cycle fatigue crack initiation and growth, which can occur at much lower stress levels, particularly in areas of stress concentration.

To address concerns relative to high cycle fatigue in the design phase of a compressor, one strategy is to avoid potential resonant conditions. This can be accomplished by maintaining separation between the forcing function frequencies and the structural natural mode frequencies thereby ensuring a resonant condition cannot exist. In other cases, either due to wide operational speed ranges or other design considerations, the possibility of running the compressor at a speed which could result in a resonant condition may still exist. In this case, the compressor design must account for the possibility of dynamic amplification and the possibility of high cycle fatigue. Analysis methods are available to predict the forcing function, damping level, resulting structural response, and assess these relative to fatigue stress allowables. The prediction of the forcing function is made using time dependent CFD simulation which includes modeling both the upstream guide vanes and the rotating impeller to capture their transient interaction. The total damping is the sum of material, mechanical, and aerodynamic damping. The aerodynamic damping is dependent on the specific geometry, gas and flow conditions and is often the largest contributor to the total damping. The prediction of the aerodynamic damping is made using a second time dependent CFD model where the movement of the impeller surfaces associated with the structural mode shape is included in the CFD simulation. The work the fluid performs on these moving surfaces relative to the structural energy in the mode shape is an indication of the aerodynamic damping. Using the time and spatially varying forcing function pressures, a harmonic structural response finite element analysis (FEA) analysis is performed with the previously derived damping level. The structural model is post processed to determine the alternating stress at the critical locations. A separate steady state structural FEA analysis with centrifugal loading is used to determine the steady stress at these same critical locations. The steady stress and alternating stress are then used in a typical Goodman diagram to assess acceptability.

This paper provides details on how to perform this type of analysis using a recent example where it was employed on a commercial centrifugal compressor.

While the work presented here is purely numerical, Lerche et al. (2010) have validated a time domain couple fluid-structure computational model for predicting dynamic blade stresses in a rotating centrifugal compressor impeller. The model was a one-way transient simulation, applying CFD-predicted pressures to a mechanical model at each time step. This approach requires that damping be specified by the analyst. Validation testing was performed with an open-loop compressor test on an unshrouded impeller with inlet guide/excitation vanes and a vaneless diffuser. The impeller was instrumented with strain gauges passed through a high gain, low noise amplifier mounted on the impeller rotor. The authors reported agreement of predictions and test data within 10%, as illustrated in Figure 1
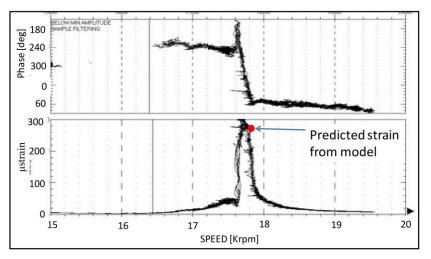
Figure 1: Comparison of experimentally measured and FSI predicted strain form Lerche et al. (2010)

EXPERIENCE USING FLUID STRUCTURE INTERACTION WITH AN INDUSTRIAL CENTRIFUGAL COMPRESSOR

A recent case considered is a multi-stage centrifugal compressor using covered impellers. The operating speed range is such that there is the potential for the frequency of the impeller blades passing through the upstream guide vane wakes may coincide with one particular impeller mode structural natural frequency. See Figure 1 for a cross sectional view of the compressor showing the stage of interest, Figure 2 for a view of the covered impeller as well as a view of the structural mode of concern.

The strength of the aerodynamic forcing function and the level of aerodynamic damping will depend upon the gas and flow conditions and is the subject of the analysis effort. For the case presented here a nominal design flow case is chosen with a gas mole weight of approximately 17 to 19 and stage inlet conditions of 200 psig and 100°F.

The specific area of concern with regard to high cycle fatigue for this impeller, and this mode shape, is the intersection of the hub and the blades near the tip of the impeller as shown in Figure 2.
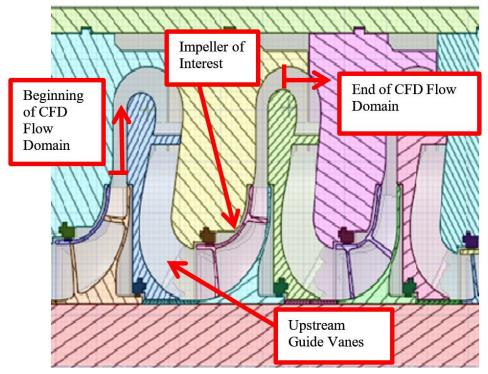

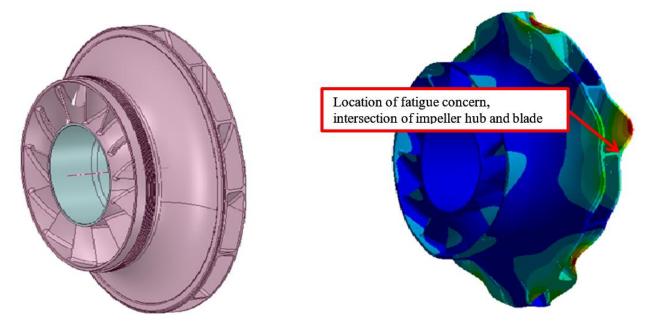**Figure 2: Centrifugal compressor stage of interest**

Figure 3: Covered centrifugal compressor and impeller structural mode shape. In the figure on the right, contour colors represent magnitude of displacement

Analysis Overview

The overall goal of the analysis effort was to assess the mechanical integrity of the centrifugal compressor with regard to fatigue associated with a single vibrational mode of interest. This work was broken into several steps. First, a static structural FEA and modal analysis was done to quantify the mode in question. Second, transient CFD was done to quantify the transient pressures. Third, an aerodynamic damping CFD study was completed to evaluate the aerodynamic damping associated with the target mode. Finally, the transient pressures and aerodynamic damping were then used to generate alternating stress values using a forced response FEA. These alternating stresses were then combined with the mean stress values to form a Goodman diagram and assess fatigue. An outline of the analysis procedure is shown in Figure 3.
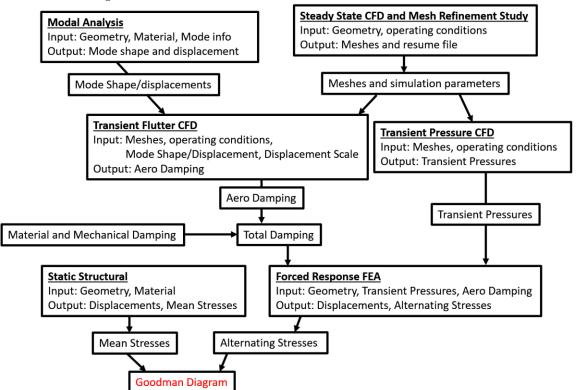

Figure 4: Overall analysis pathway to arrive at the Goodman Diagram for the target mode.

Computational Fluid Dynamics Analysis of Transient Pressures
In order to quantify the unsteady pressures on the impeller for use in the forced response analysis, a transient CFD study was needed. To ensure that the meshes used for this study were appropriate, first a steady state, single passage, CFD model was used to measure the effect of mesh size on the solution and to verify the overall stage performance was in line with the expected values as indicated by benchmarked equipment supplier predictions. The model included detailed meshing of the front and back cavities as well as the impeller flow field itself along with upstream guide vanes. To ensure that the results could be mapped directly to the structural model, the same geometry was used to create the structural mesh as the fluid mesh including blade fillets/chamfers, which are often ignored for aerodynamic only CFD simulations.

Traditionally, in order to obtain the transient pressure data required for the forced response analyses a full 360 sliding mesh CFD model would be needed. The domains used for this type of model are shown in Figure 4.
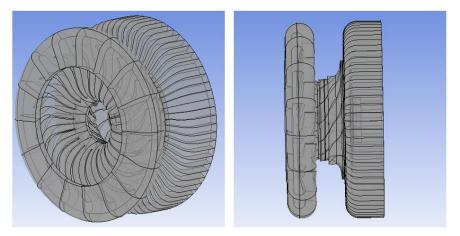

Figure 5: Domains Used for Transient Full 360 Sliding Mesh Analysis

As is shown in Figure 4, the model includes all the rotor passages as well as each of the upstream guide vanes. During the simulation, the rotor mesh is rotated relative to the guide vane mesh and the time accurate pressure field on the rotor surface is generated. Although this simulation method accurately models the interaction between the rotor and the stator, due to the large number of passages required, this type of simulation is computationally very expensive.

Alternatively, the transient CFD solution can be efficiently performed by taking advantage of the periodic geometries of the guide vane and the impeller regions and modeling them as separate domains. At the interface between the guide vane and impeller domains, which have different numbers of blades per circle, a pitch change model must be employed. One ANSYS CFX pitch change solution method to perform this calculation is the Fourier Transform (FT) Method.

In the FT method the periodic nature of the problem, i.e. each vane passing is identical to the last, allows the solution variables at each point in the domain to be decomposed into harmonics of the fundamental blade passing frequency using a Fourier series. Note an alternative solution method not chosen in ANSYS CFX is the time transformation, which would require several more passages be modeled due to the restrictions on allowable pitch ratio being nearer to 1.0. The Fourier Transformation method in ANSYS CFX is implemented using two stator and two rotor passages. See Figure 5 for a view of example CFX domains.
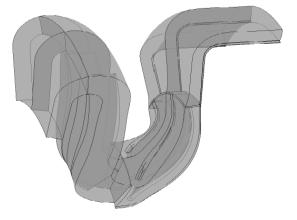

Figure 6: Domains Used for the Fourier Transform Method.

In the FT method, the coefficients of the Fourier series are determined by carrying the solution in domain specific time, updating the value of the coefficients at each time step, until the solution converges to a solution which is periodic in time over the blade passing period. Note that due to the differences in pitches the impeller domain time step is larger than the guide vane domain time step. The solution normally will take a number of blade passing periods to converge. By default ANSYS uses seven harmonics at 1X blade passing, 2X blade passing, 3X…..7X blade passing to describe the time variation of the solution variables. As the CFX solution marches forward in time, at each time it has a new updated set of harmonic coefficient values, which support the current time's values as reconstructed from all of these coefficients. At certain user chosen monitoring points the time history of the results, such as pressure, is maintained. Convergence is judged based on the time history of these monitored values becoming the same over the current blade passing period as the previous blade passing(s) within a user chosen tolerance. Note the forced structural response analysis is driven by the 1X blade passing content, therefore only the 1st harmonic content was extracted from the 7 harmonics solution to apply to the structural harmonic response model.

Regardless of the method used, the results of the simulation are the magnitude and phase of the transient pressures on the rotor surface at the frequency of interest which is what is needed for the forced response FEA. In the case of the full 360 model time transient, an FFT can be used at each point on the rotor surface to extract the magnitude and phase of the alternating pressure signal. Figure 6 shows the normalized magnitude of the alternating pressure on the rotor surface for the target frequency.
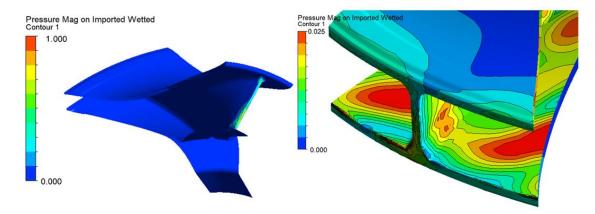

Figure 7: Normalized Magnitude of Alternating Pressure.

As is shown in Figure 6 on the left, the highest alternating pressure magnitude on the impeller is on the blade leading edge. The OD of the impeller, which is the area of interest for the target mode for this study, had considerably less pressure fluctuation. The magnitude and phase of the rotor surface pressure data is used as an input for the forced response analysis which will produce the alternating rotor stresses.

Computational Fluid Dynamics Analysis of Aerodynamic Damping
Along with the transient pressures, the aerodynamic damping is also needed for the forced response analysis and can be estimated using a CFD moving mesh simulation to predict the aerodynamic damping for the target mode and operating conditions.

ANSYS CFX is able to predict aerodynamic damping for a particular mode by imposing the mode shape on a moving wall CFD simulation and then measuring the resulting aerodynamic work. The first step of this process is exporting the normalized mode shape from an ANSYS mechanical modal FEA performed previously. This mode shape is then imported into CFX. For the present study the normalized mode shape was scaled to provide a maximum modal displacement of half of the radial clearance between the impeller tip and the stationary component. Although basing the value is not a value driven by aerodynamic response characteristics, if the axial and radial maximum displacements were equal, it would be in line with what might be considered an allowable maximum response. As has been demonstrated by other analyses, the resulting predicted magnitude as described by percent of critical damping is largely independent of the exact maximum modal displacement applied. For the inlet boundary condition, the full 360 steady state results were circumferentially averaged at the return channel outlet and this velocity profile was imposed at the impeller inlet. The rest of the boundary conditions were the same as in the transient sliding mesh CFD study discussed previously. An image of the domains used for the simulation is shown in Figure 7.
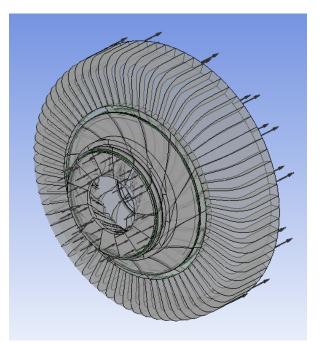
Figure 8: Domains Used in Aerodynamic Damping Calculation

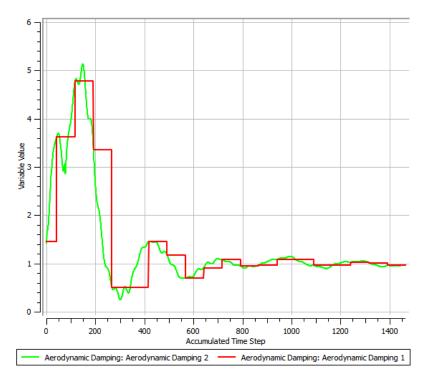Figure 8 shows the convergence history of the computed aerodynamic damping.

Figure 9: Aerodynamic Damping Monitors. In this figure, values are normalized to the final calculated value. Aerodynamic damping 1 is the value as calculated from the previous number of time steps equal to 1 blade passing, updated at each time step while aerodynamic damping 2 is the value as calculated from the previous number of time steps equal to 1 blade passing, updated at the completion of each blade passing cycle.

As is seen in the image, the aerodynamic damping monitor converged to a steady state value after approximately 1400 timesteps. The resulting wall power density at a snapshot in time is shown in Figure 9. The wall power density is the rate at which work is being performed by the fluid on the impeller walls. The integral of the wall power density over the impeller surface and through one mode cycle in time is the aerodynamic work per cycle. This work is in effect what creates the aerodynamic damping.
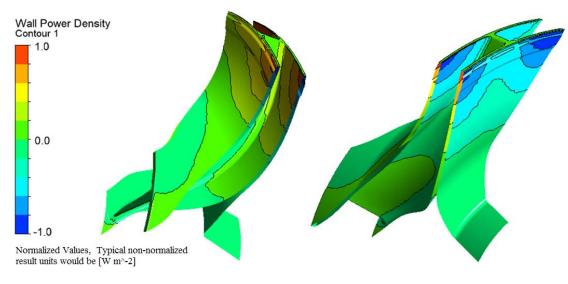
Figure 10: Wall Power Density

The percent of critical damping is needed for the forced response structural FEA model. This was computed using the following equation:

$$\zeta = \frac{W}{(4*\pi*Umode)} = \frac{W}{2*\pi*\omega^2*\left[\frac{CFD\ \max\ displacement}{FEA\ modal\ \max\ displacement}\right]^2}$$

In this equation, ζ is damping as a ratio to critical damping, W represents the aerodynamic work per cycle which is an output of the CFD model, Umode is the structural energy contained in the mode and ω is the frequency of the mode in cycles per second. The ratio of CFD max displacement to FEA modal max displacement is used due to the normalization done in the ANSYS export of the structural mode shape for use by CFX.

Structural Modeling

While many new impellers are one-piece construction, without welds, some percentage continues to be welded due to geometric or other factors. Also, the vast majority of impellers currently operating in the field are of welded construction. The subject impeller is a two-piece construction, with the blades integral to the cover and the blades attached to the hub by welding. The location where a crack is most likely to initiate due to stresses associated with the structural mode shape of interest is at the weld toe. The solid model of the impeller used for FEA is a sector containing one blade, which has the same cut boundaries as the fluid model, as shown in Figure 10.
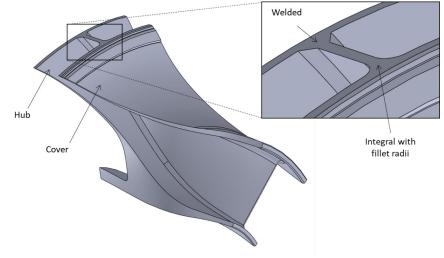

Figure 11: **Solid Model of Impeller Sector**

Structural Modal Analysis

A modal analysis of the impeller is performed, and the mode eigenvalues (frequencies) and eigenvectors (shapes) are obtained. In this case, there is one particular mode of interest due to its frequency and shape aligning with a possible excitation, namely 1x upstream guide vane wake passing at a specific speed and in the 3rd nodal diameter pattern. The mode shape is as shown in Figure 2. This mode shape is used as input to the prediction of aerodynamic damping as discussed previously.

Steady-State Structural Analysis

Steady-state structural analysis of the impeller was performed with centrifugal loading associated with the rotational speed of the impeller. As a check, a modal analysis was also performed on the pre-stressed impeller to confirm the agreement of the original modal analysis' result. Pre-stressed here meaning the forces, stresses and strains due to the centrifugal loading are included in the modal analysis providing some additional stiffening of the structure. The first three-nodal diameter (ND3) mode's frequency agreed within 0.5% when including the pres-stress vs. without. The bulk stress and deflection results are typical and are not presented for brevity. These steady stresses are used in the final Goodman diagram evaluation.

Structural Model Post-Processing

Where the blade is integral to the cover, there are fillet radii, but where the blade is connected to the hub, the weld is modeled as a chamfer with sharp transitions to the blade and hub. Due to the sharp corner in the model, it was not possible to achieve a mesh-independent solution of the nodal stresses at that location. The actual geometry at the toe of the weld is really not known exactly due to variations inherent in the welding process. Typically, structural evaluations of fatigue design for welded components are correlated to a structural, or more general, stress that is independent of the exact detail of the weld toe corner. In this work, two alternate metrics were used to evaluate stress: linearized stress and hot spot stress.

Linearized stresses are evaluated along a path through the material, and the stresses along the path are characterized by the membrane (uniform along the path), bending (first-order variation along the path), and peak stresses (higher-order effects). For this case, the path would be from the toe of the weld on the flow path side of the hub through to the back side of the impeller. The peak stresses would capture the "unbounded" nodal stress at the toe of the weld, while the membrane and bending stresses would not and, therefore, would be able to achieve mesh-independent values. Commercial standards such as the Eurocode 3 (2005) use the type of weld detail and the structural stress to enter a fatigue curve in order to determine the allowable number of stress cycles. The structural stress is the stress in the attached component as would be calculated using forces, moment, and member section properties. The linearized membrane plus bending stress normal to line of the weld, as obtained from an FEA model, is equivalent to the structural stress.

The hot spot stress is analyzed by extrapolating stresses near the toe of the weld to determine the value at the toe of the weld – i.e., stress "hot spot". Because the nodal stresses away from the toe of the weld (sharp corner) can achieve mesh-independent values, the hot spot stress would also be mesh-independent. Orr (2008) described the details of the hot spot stress analysis method for an impeller fatigue analysis and presented the following definition for calculating the hot spot stress value:

$$\sigma_{HS} = 2.52\sigma_{0.4t} - 2.24\sigma_{0.9t} + 0.72\sigma_{1.4t}$$

Here, σ_{HS} is the hot spot stress value, $\sigma_{\alpha t}$ is the stress component normal to the axis of the weld on the surface a distance αt from the toe of the weld ($\alpha = 0.4, 0.9, 1.4$), and t is the thickness of the hub. Figure 11 illustrates these definitions. A grid of these stress evaluation points was created by splitting the surfaces of the solid model in order to create vertices for which the FEA results could be extracted. Since the location of the peak hot spot value was unknown *a priori*, multiple locations at different radii were evaluated. Figure 12 shows the grid of points created on the solid model.
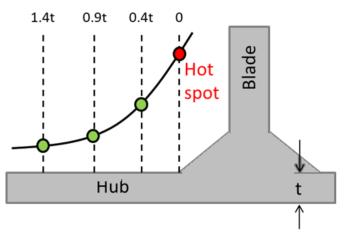
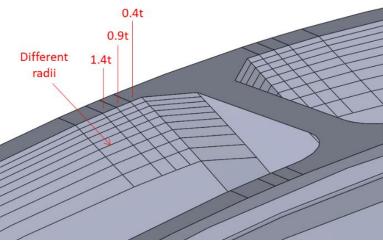**Figure 12**: **Stress Locations for Hot Spot Stress Evaluation**

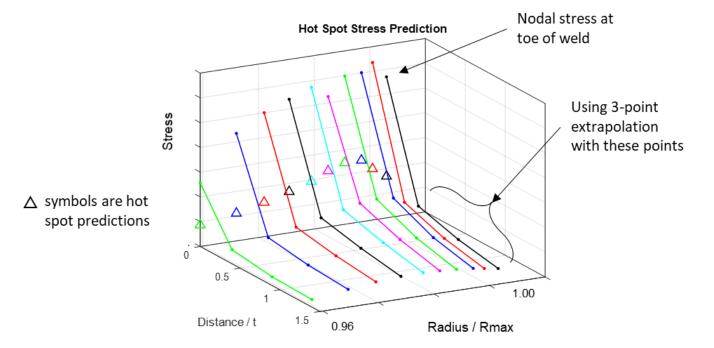**Figure 13**: **Hot Spot Stress Locations Applied to Current Impeller**

Figure 14: **Nodal Stresses and Hot Spot Stress Prediction for Static FEA Result**

Figure 13 shows the nodal stresses and hot spot predictions for the different radial locations identified in Figure 12 . The nodal stresses at the toe of the weld are shown only for comparison relative to the predicted hot spot stresses. The peak hot spot stress appears slightly within the maximum radial position.   Figure 14 shows the comparison of the hot spot stress values (same as shown in Figure 13) and the maximum linearized stress (membrane plus bending) for the static FEA results. As opposed to the hot spot stress, the peak linearized stress occurs at the outer diameter and is about 8% lower magnitude.
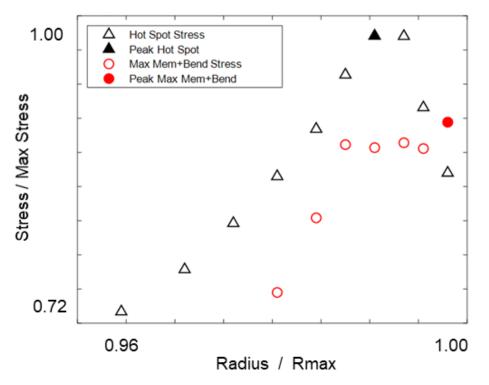

Figure 15: **Comparison of Hot Spot Stress and Maximum Linearized Stress for Static FEA Result**

Forced Response Analysis

Forced response analysis was performed implementing an ANSYS-built application, developed specifically for use with cyclic symmetric models such as bladed disks, impellers, etc. The analysis is coupled with the modal analysis results. The complex pressures from the transient CFD simulation (i.e., magnitude and phase of the forcing function) were applied to the wetted impeller surfaces, and the frequency response of the system was performed over a range of approximately ± 5 Hz from the expected peak response. A damping ratio equal to the estimated material damping, was used. The peak stress amplitude at resonance from the forced response analysis occurred in a different location than the peak mean stress – it occurred on the blade side of the weld, but it was still at the toe of the weld. As with the static analysis results, the peak values of the forced response results occur at a sharp corner, so these nodal results are unreliable. The hot spot stress extrapolation method was employed to evaluate these areas (more conservative than linearized stresses, see Figure 14). To make comparisons to the case with material plus aero damping, the stress results were scaled by the linear system assumption that peak response at resonance is inversely proportional to damping.

Fatigue Strength Assessment

Fatigue assessment is typically carried out by plotting alternating stress amplitude vs. mean stress on a Goodman diagram. The main boundary line on the Goodman diagram connects the endurance limit plotted on the zero mean stress axis with the ultimate tensile strength plotted on the zero alternating stress axis. The second boundary line (not always used in fatigue analysis) connects the yield stress plotted on both axes.   Key in defining the Goodman diagram is the endurance limit. This is the allowable alternating stress below which no fatigue failure will occur. This is applicable to the case under consideration due to the very large number of cycle, reaching on the order of 10^{10} stress cycles per year of compressor operation. To define the endurance limit, consideration of fatigue design curves is given with an eye toward the high cycle portions of the curve.

Several references were consulted to determine the appropriate S-N (fatigue stress vs. cycles to failure) curve to use for this

application. Orr (2008) presented a method to calculate hot spot stresses for a welded impeller fatigue analysis. Eurocode 3 (2005) is a European standard on welded structure design, which is applicable to welded steel structures with stresses determined by the hot spot approach. Maljaars et al. (2013) is a commentary on the Eurocode. Lassen and Recho (2006) is a book on the fatigue of welded structures. Finally, sections of the ASME Boiler and Pressure Vessel Code (BPVC) were also referenced. The following conclusions were made from the collective review of these sources:

- Fatigue of wrought material normally comprises cycles to initiate a crack, followed by cycles to grow the crack. However, a weld already contains micro-cracks; therefore, fatigue of welds only involves crack growth.

- Crack growth of steels is relatively constant, regardless of steel type or material strength. As a result, the codes present S-N curves that are applicable for steels and stainless steels, and the slope on a log-log plot (i.e., the exponent of the power function) is the same. In other words, stress is proportional to the number of cycles to the B power, where B is -0.3195 (ASME) or -1/3 (Eurocode 3) for all steels and stainless steels.

- The amplitude of the S-N curve is a function of the weld geometry configuration only, which is effectively a characterization of the typical stress loads on the weld. For example, Eurocode 3 provides a table that specifies the value of stress at 2e6 cycles based solely on the type of weld construction. There is no reference to material type or strength.

Scaled S-N Curves

The team had access to fatigue test data of weld samples cut from a similarly-constructed impeller in order to characterize fatigue life in a previous project. The fatigue curve shown in Figure 15 represents a curve constructed with the slopes presented by the Eurocode 3 standard and the amplitude scaled to fit the previously measured failure data. The resulting cutoff limit, or endurance limit, is then taken from resulting curve at very high number of cycles ($>10^8$).
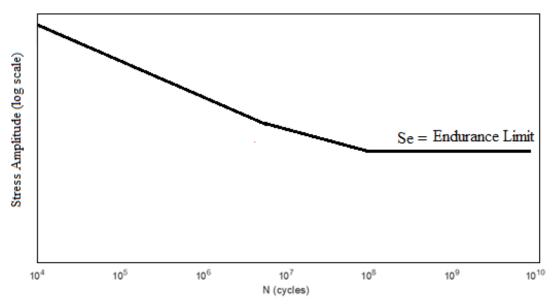

Figure 16: **Scaled S-N Curves Based on Previous Fatigue Data and Eurocode Slopes**

Goodman Diagram

Figure 16 shows a Goodman diagram for the first ND3 mode. The endurance limits shown represent the cutoff limits from Figure 15. The up- and down-pointing triangle symbols represent the evaluated hot spot stress points, corresponding to the maximum mean stress and maximum alternating stress locations, respectively. The points are within the boundaries in the Goodman diagram and are acceptable.
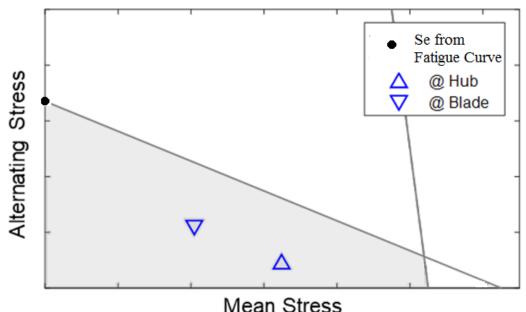
Figure 17: Goodman Diagram for Stresses Corresponding with First ND3 Mode

CONCLUSIONS

Current analysis tools allow the prediction and evaluation of flow induced mechanical vibration of covered centrifugal compressor impellers. The case study presented starts from the compressor stage operating parameters and geometry and results in a prediction of the steady and vibratory stress fields in the impeller. Special attention is given to the post processing of the predicted stress field and its interpretation with regard to a Goodman diagram for assessment of acceptability with regard to high cycle fatigue. The techniques can potentially be applied to the assessment of new equipment or to aid in the failure analysis of an impeller which has experienced damage. In the failure analysis case the methods can identify a concern relative to flow induced high cycle fatigue or rule it out, allowing attention to be focused on other possibilities, such as operational issues including high levels of entrained liquid or operation near surge or deep choke.

REFERENCES

Lerche, A., Moore, J. J., & Feng, Y. (2010). Computational modeling and validation testing of dynamic blade stresses in a rotating centrifugal compressor using a time domain coupled fluid-structure computational model. In *ASME Turbo Expo 2010: Power for Land, Sea, and Air* (pp. 799-807). American Society of Mechanical Engineers Digital Collection.

Orr, S., 2008, "Impeller Fatigue Assessment Using an S-N Approach," Paper No. 5244-08, AMCA International Engineering Conference, Las Vegas, March 2-4.

Eurocode 3, EN 1993-1-9, 2006 "Design of steel structures – Part 1-9: Fatigue".

Lassen and Recho, 2006, Fatigue Life Analyses of Welded Structures, Ch. 2: "Basic Characterization of the Fatigue Behavior of Welded Joints," Ch. 5: "The S-N Approach," Wiley.

Maljaars et al., 2013, "Comparison Between the Eurocode for Fatigue of Steel Structures, EN 1993-1-9, and the Eurocode for Fatigue of Aluminium Structures, EN 1999-1-3," 5th Fatigue Design Conference.

Boiler, A. S. M. E., and Pressure Vessel Code. "Section VIII, Division 1-Rules for Construction of Pressure Vessels." Amer. Soc. Of Mech. Eng., New York (2007).